ASTFE American Society of Thermal and Fluids Engineers

Proceedings of the 2nd Thermal and Fluid Engineering Conference, TFEC2017
4th International Workshop on Heat Tr: SAND2016-10176C
April 2-5, 2017, Las Vegas, NV, USA

TFEC-IWHT2017-17709

CONTAMINATED FUEL FIRES: PARAMETRIC SENSITIVITY OF RESUSPENSION AND BOILING PARTICLE EVOLUTION

Ethan T. Zepper[1*], Alexander L. Brown[1], Flint Pierce[2], Tyler Voskuilen[2], and David Louie[3]

[1]Fire Science & Technology Dept., Sandia National Laboratories, Albuquerque, NM 87185-1135, USA
[2]Comp. Thermal & Fluid Mech. Dept., Sandia National Laboratories, Albuquerque, NM 87185-0836, USA
[3]Severe Accident Analysis Dept., Sandia National Laboratories, Albuquerque, NM 87185-0836, USA

ABSTRACT

The safety requirements for handling hazardous materials are important, as they dictate costs and designs associated with related facilities and operations. One such concern relates to respirable hazards that sometimes can become mixed with a flammable solvent (i.e., gasoline) and ignited. As part of maintaining health, safety, and security, the U.S. Department of Energy (DOE) maintains a number of documents to ensure safety across the DOE complex. A DOE Handbook (DOE-HDBK-3010) provides boundary estimates for various accident types, including fire, explosion, and seismic events. These estimates allow safety analysts to incorporate hazards in evaluating safety systems to protect people in the event of an accident of this nature. The basis for the recommendations relates to historical tests. Current computing capabilities offer new methods to assess the hazards. In the interest of updating and assessing the DOE handbook recommendations, we are re-visiting historical experimental tests and modeling the scenarios. This paper focuses on a historical test where a gasoline pool fire was doped with a solid contaminant. To better simulate this scenario, we have implemented some new capability in our simulation codes. We have added a multi-component evaporation model, and we have developed a model for particle adhesion and re-suspension. The new capabilities contribute to the understanding of the physical tests. We identify the duration of the active boiling regime to be the most critical parameter to the quantitative outcome of the predictions. The newly implemented model capabilities are important code improvements that allow models to better predict the physics of this type of scenario.

KEY WORDS: Computational methods, Particle entrainment, Computational fluid mechanics, Fire, Contaminant release, Airborne release, Safety

1. INTRODUCTION

Consider transportation accidents of vehicles transporting radioactive material in which the powder or particulate is immersed in the fuel or flammable solvent. There is a health danger from potential radiological releases through the entrainment of particles into the air, particularly those particles in the respirable range (<10μm). Such an accident is a realistic health threat in the nuclear power and processing industry.

Safety guidelines for determining potential releases for such an incident are provided by the U.S. Department of Energy (DOE) in a handbook, DOE-HDBK-3010 (DOE, 2013). The handbook provides estimated airborne release fractions (ARF) and respirable fractions (RF) for use by safety analysts assessing the incident hazards. The release fraction is calculated as the ratio of entrained contaminant mass to total contaminant mass. The ARF values provided in the handbook are mostly based on experiments performed between 1960 and 1980. Many experiments were performed on a smaller scale than the potential threat, and therefore may not provide direct insight to realistic events. Modern computational tools exist that can

*Corresponding Author: etzeppe@sandia.gov

provide release fraction predictions with increased fidelity, and can be applied to a broader selection of scenarios. An experiment performed by Mishima and Schwendiman (1973) was simulated using Computational Fluid Mechanics (CFD) software where various contaminants were suspended in a mixture of kerosene and 30% trybutal phosphate (TBP) in a 50 mL beaker (Mishima and Schwendiman, 1973, Brown and Louie, 2015, Louie et al., 2015).

In addition to the beaker fire simulations, larger scale simulations were done on an experiment focusing on particle entrainment from a gasoline pool fire contained in a wind tunnel (Mishima and Schwendiman, 1973, Brown et al., 2015a). This experiment is more germane to a potential transportation accident because pool fires generally transition from laminar to turbulent as the diameter increases approximately past one meter (Drysdale, 1998). The SIERRA/Fluid Mechanic (FM) code Fuego was used to perform the beaker and gasoline fire simulations (Sierra Thermal Fluids Development Team, 2016). Several modified scenarios were also investigated to account for uncertainties from the reported physical experiments and to determine parameter sensitivities.

Additional physics have since been implemented into the code suite to support the improved modelling capability for these scenarios, prompting reanalysis of both previous simulations. The added capabilities included the ability to specify multiple species components in a single particle and track volatile evaporation and individual species deposition onto boundaries. A model to adhere and subsequently resuspend particles 'stuck' on boundaries was also implemented. This paper describes the Fuego simulation comparisons of the gasoline pool fire experiment with the experimental results, as well as the previous simulated results (Brown et al., 2015b). The goal of this effort is to determine the impact magnitude that the inclusion of multi-species tracking and resuspension has on the previous predicted results.

2. THEORY

2.1 Entrainment Mechanisms

For pool fire scenarios, four particle entrainment mechanisms shown in Table 1 were identified from the literature to be potentially active during fires of this nature. A more detailed description of the meaning and justification for these phenomena is presented in previous work (Brown et al., 2015b).

Table 1 Entrainment mechanisms believed potentially active in this scenario.

Mechanism	Conditions for Activity	Parametric Functional Sensitivity	References
Evaporation Induced Entrainment (EIE)	Liquid is actively evaporating	Particle size distribution Density Exposed Surface Area Rate of evaporation Vapor pressure of the solvent Evaporating species molecular weight	(Mishima and Schwendiman, 1968)
Surface Agitation by Wind	Existence of a substantial wind and a liquid surface	Wind Speed Surface Tension Viscosity Density Fire dimensions Fuel layer depth Geometry present	(Derakhti and Kirby, 2014)
Surface Agitation by Boiling	Pool temperature approaches boiling point of liquid	Rate of Boiling Size of bubbles Viscosity Surface Tension Density	(Mishima and Schwendiman, 1973, Kogan and Schumacher, 2008, Bagul et al., 2013, Borkowski et al., 1986, Kataoka and Ishii, 1983)
Residue Entrainment (Resuspension)	Wind , vibration, or other activating factors, and no remaining liquid	Wind Speed Particle sizes Density Viscosity Particle forces	(Roberts et al., 2003, Lick, 2009, Sehmel, 1984, Henry and Minier, 2014, Young, 2015)

Evaporation induced entrainment (EIE)

The fuel pool consists of gasoline that will evaporate at ambient conditions. Evaporation is enhanced by the presence of the fire. Despite the liquid temperatures being well below the evaporation temperature of the contaminant, releases have been observed in prior testing of this nature (Kogan and Schumacher, 2008). The mechanism driving this release is not completely clear. It likely relates to the momentum or energy carried by evaporating gases imparted onto the smallest non-volatile contaminant near the pool surface. This is the source of the name 'evaporation induced entrainment'. This mechanism was observed in the previous work (Mishima et al., 1968).

Surface agitation by wind

This mechanism entrains particulates through surface instabilities and wind related disturbances. This process does not require a fire to be active, rather a strong wind flowing across a fuel pool surface can agitate the liquid and create waves. A frothy layer of mixed liquid and gas fuel can form along with pinching of wave tips, both with the possibility to entrain contaminant. A detailed description of this mechanism and contributing components can be found in previously presented work (Derakhti and Kirby, 2014).

Surface agitation by boiling

This mechanism is studied more extensively. It is particularly active in deep pools near the boiling temperature and shallow pools at near burn-out conditions. It begins with the formation of bubbles in the pool which rise and rupture at the liquid surface. Previous work focused primarily on this mechanism, as the experiment being simulated was designed to highlight this entrainment mechanism (Mishima and Schwendiman, 1973, Brown and Louie, 2015, Louie et al., 2015). Work done by Borkowski et al. (1986) provided the basis for the particle size distribution, while the superficial evolution was determined from correlations of Kataoka and Ishii (1983). The equations used to determine source terms for the below scenario are presented in detail in the previous work (Brown et al., 2015a). This study observed that the model predicted that the boiling mechanism was significantly dominant over the evaporation induced entrainment mechanism. The correlations used are thought to be applicable to problems insofar as the materials are similar to boiling water, which was used to develop the fit parameters

Residue entrainment (resuspension)

Resuspension of particles adhering to surfaces may have a significant contribution to the overall ARF. Resuspension occurs as air flows across a particle laden surface, and the lift force experienced by the individual particles overcomes the adhesion and gravitational forces. The resuspension model is based on work done by Wichner and summarized by Young (2015). The equations used in the force balance are the following:

$$F_{lift} = \alpha A_p \tau_w \tag{1}$$

and

$$F_{adh} = 10^{-9}\frac{r}{\varepsilon} \tag{2}$$

where F_{lift} is the lift force on the particle, α is a lift coefficient, τ_w is the wall shear stress, F_{adh} is the adhesive force on the particle, r is the particle radius, and ε is the surface roughness. The gravitational force acting on the particle is also included in the force balance this model. The validation of the resuspension model is as yet incomplete.

2.2 Multi-Component

In the experiments, the contaminant was dispersed in the fuel. Assuming the boiling mechanism is dominant, entrained particles will be a combination of both the fuel and the solid contaminant. The solid contaminant is non-volatile as it's melting temperature exceeds temperatures experience in this system by approximately 800 °C. It is suspended in the evaporating fuel droplet. Due to the fact that the fire was generally well above the boiling temperature of the fuel, the liquid phase fuel in the entrained particles evaporates rapidly, leaving the smaller contaminant particles entrained in the fluid flow. With the multi-component particle model (Pierce et al., 2016), particles can evaporate volatile components separately. Particle diameters are reduced through fuel evaporation, resulting in just the trace contaminant once the fuel fully evaporates. Particles interacting with the boundaries deposit components accounted for separately for individual species deposition analysis.

3. METHODS

Simulations of historical tests are made feasible by combining components of the models described above in the theory section. This section describes the CFD capabilities and parameters used to perform simulations on the gasoline pan fire experiments performed by Mishima and Schwendiman (1973). New interpretation of the experimental effort is obtained as the simulations provide higher fidelity insight into the various contributing phenomena and their relative importance to the overall solution.

3.1 CFD Capabilities

Simulations were performed using the SEIRRA/Fluid Mechanic (FM) predictive code suite allowing multi-physics on the parallel computing resources available at Sandia National Laboratories. The suite tool Fuego was employed for calculations. Fuego is a low Mach number code suited for flow, fire and particle dynamics simulations. It solves the Naiver-Stokes equation for reacting flows. For the calculations presented here, the TFNS turbulence model (Magnussen, 1981) was selected, as was the EDC reaction model (Tieszen et al.,2005). Particles were simulated with a Lagrangian/Eulerian two-way coupling scheme between the fluid and particles.

3.2 Experimental Conditions

Simulation parameters were based on sub-tests SA-17a and SA-17b from Mishima and Schwendiman (1973) experiments. In SA-17a, particles were released from a gasoline pool fire contained within a wind tunnel with a flow of less than four miles per hour. Depleted uranium dioxide (representing plutonium) was distributed by hand into the 15-inch diameter stainless steel pan, prior to the addition of gasoline. One gallon of gasoline was added via a nozzle directly above the pan, and subsequently ignited. High Efficiency Particulate Air (HEPA) filters collected the entrained contaminants during the nine-minute burn. The filters were removed after burnout for analysis. For experiment SA-17b, the filters were replaced and the flow resumed for 4.7 hours, after which the filters were again removed for analysis.

3.3 Input Boundary Conditions

From the previous work it was determined that, while present for the majority of the burn, EIE is not a significant contributing entrainment mechanism when compared with the release values predicted from the boiling mechanism. A visual representation of the model prediction during the boiling phase is seen in Figure 1. The boiling mechanism is initiated near the end of the burn as the pool begins to boil. The precise boiling onset time for the experiment simulated here is unknown, as it was not recorded in the physical experiment. Particle source terms are determined from correlations and are based on similar experiments in the literature. Previous Fuego simulations employed a one-dimensional pool model to represent the evaporation of the gasoline in the steel pan. During the boiling phase, the evaporation of the particles will be a major contributor to the gas fuel source term. The magnitude of this was estimated, and the pool boundary condition was modeled with a fuel source term equal to the steady-state burn rate minus the estimated particle fuel source term.

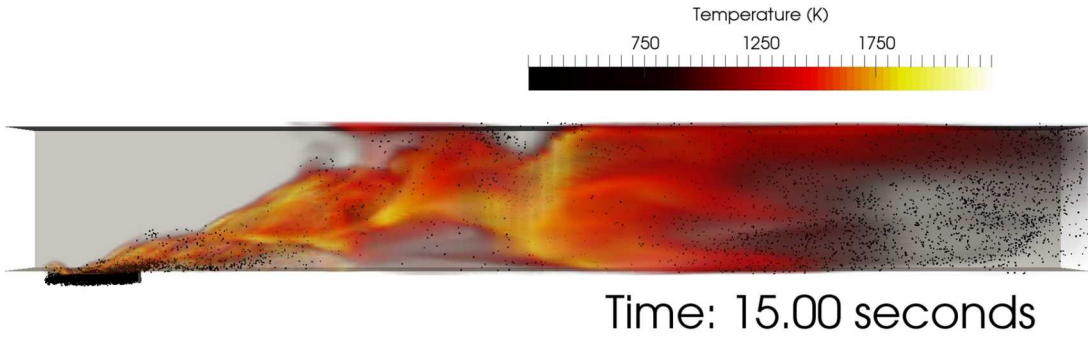

Fig. 1 Boiling scenario: Contaminant entrainment prediction, parcels enlarged for visualization.

Resuspension of contaminants was of interest in the original physical experiment, and the code suite now has the model framework to predict resuspension. As of this publication, the multiple species particle evaporation and tracking capability were not integrated into the same version of the code as the resuspension model; therefore, the simulation particle parameters were reverted to be identical to those assumed in the previous work. This included using the one-dimensional pool model. Contaminants were released in a fire, and allowed to deposit on boundaries using the new particle deposition model. After burn-out, the input air flow remained, and the particles were allowed to resuspend in this flow.

Mesh specifications.

A wind tunnel mesh, unchanged from mesh in the previous work, was generated using the experimentally reported dimension, as seen in Fig. 2. The wind tunnel is modelled at 4.57 m long with a .66 m square cross-section. Surface 1 is the air inflow boundary, with a fixed flow rate of 1 m/s (2.2 mph, assumed from the test report). Surface 2 represents the stainless steel tunnel walls, modelled with a 1.3 cm conducting wall boundary condition. Surface 3 is the outflow boundary condition placed near the experimental filter location, set to collect entrained particles. Surface 4 represents the dirt ring in which the fuel pan is set, modelled as a 1.3 cm thick 1D conducting surface. Surface 5 represents the fuel pan. The circular pan measured 0.381 meters in diameter, and assumed in the model to be filled with pure heptane fuel (C_7H_{16}) as a surrogate for the gasoline used in the physical experiment. Heptane liquid and the gas phase thermodynamic properties represent the more complex gasoline fuel mixture used in the experimental test. Finally, surface 6 is the exposed lip of the stainless steel pool, modelled as a conducting boundary condition.

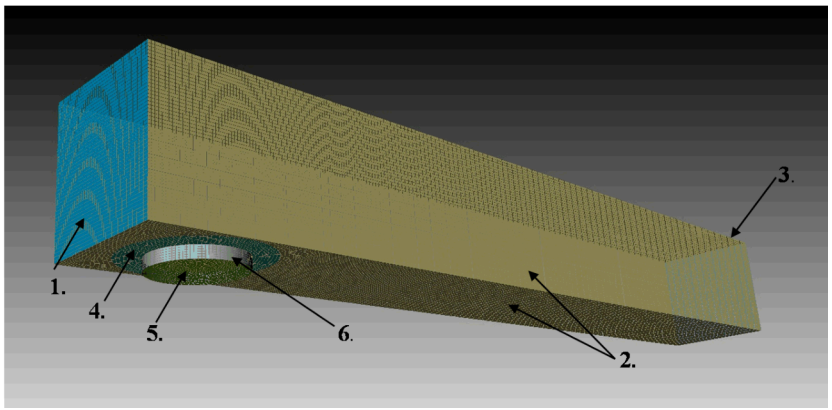

Fig. 2 Wind tunnel mesh: Geometry and surfaces.

Previous work simulated two different lip heights to account for the "near-full" and "near-empty" fuel height conditions. This work only uses the "near-empty" mesh, as that corresponds best to the boiling and resuspension mechanisms. The lip height was set to 51 mm, and multiple mesh refinements were made to determine mesh convergence. Minor variations between simulations using the above described mesh and simulations involving further refinements indicated that baseline mesh exhibited adequate mesh convergence. It was therefore selected as a baseline. The mesh was relatively uniform with 12.7 mm spacing near the fuel pan, and increased spacing downstream to improve the computational speed. The baseline mesh had 709,856 elements.

To determine the mass deposition on various boundaries, the mass deposition density for each surface is integrated at the end of the simulation. The simulations were run for 5 seconds past the last particle injection time to account for settling of suspended particles. Particles are permitted to deposit on the walls, pool, lip, dirt ring and outflow of the tunnel. Both species (fuel and UO_2 contaminant) are integrated separately.

Turbulence parameters

Precise turbulent boundary condition parameters could not be gathered from the experimental report and this therefore was treated as a free parameter. It was assumed that a grate would be present to protect against large foreign objects entering the blower, so 10 cm was chosen as a length scale. The base turbulence intensity was set to 20%, but, due to the experimental uncertainty, it was increased in one scenario to 100% to study the effect on entrainment. The turbulence was modelled using TFNS, which is a hybrid LES-RANS model (Magnussen, 1981). The turbulence parameters used are listed below in Table 2. K is the turbulent kinetic energy and ε_{turb} is the turbulent dissipation parameter.

Table 2 Turbulent boundary conditions for surfaces and scenarios.

Turbulence Location	K	ε_{turb}
Inflow Boundary Surface (1, Fig. 2)	2.0×10^{-2}	4.64×10^{-3}
Pool Surface (5, Fig. 2), not Boiling	1.13×10^{-6}	1.12×10^{-6}
Pool Surface, Boiling	3.11×10^{-4}	1.23×10^{-4}
Inflow Boundary, 100% Turbulence Intensity	5.0×10^{-1}	9.7×10^{-1}

Pool model

The fuel pool was modeled using a fuel vapor injection velocity. Gaseous fuel is injected into the system at the surface of the fuel pan at a constant rate. The injection rate is estimated from the steady-state burn rate minus the amount of fuel located in the particle injections. Prior to the injection of particles at 3 seconds, the vapor velocity was 0.013 m/s. The flow rate was reduced to 0.00389 m/s to compensate for the evaporating fuel from the entrained particles. After particles injections ceased, the velocity was reduced to 0.0013 m/s to represent near burnout conditions.

Particle injection method

Particle parcels are introduced to the simulation through an input data file. This file contains parameters for position, initial velocity, temperature, diameter, particles represented by a single parcel, and the injection time of each parcel. The parcels are randomly distributed across the pool area and sized based off a distribution (Borkowski et al., 1986). The particles are assumed to be solid UO_2 contaminant suspended in a fuel droplet. The droplet mass fractions of heptane and uranium dioxide contaminant were chosen to be 0.98 and 0.02 respectively, based off of the pool mass fraction. The injection height was fixed at 10 mm off the pool surface for the base scenario, and parcels were given a random velocity normal to the pool. The particles were birthed at an assumed temperature of 370 K, one degree lower than the boiling point. Quantitative grounds for injecting particles are outlined in the above sections.

Radiation boundary conditions

The radiation boundaries were modeled with an emissivity of 0.9. Emissivity and absorptivity are assumed to be equal through Kirchoff's law. The tunnel wall material was modeled as stainless steel using a 1D conduction model.

Particle boundary conditions

All surfaces in the multi-component boiling scenarios were assumed to be 'stick' boundaries, which collect particles that collide with that boundary. Species mass, total deposited mass, and number of particles represented per parcel are recorded on the boundary nodes. The resuspension scenario employed the general resuspension boundary that calculates a force balance on collided particles to determine if they adhere. Subsequently, the force balance is applied to adhering particles to determine if they will resuspend into the flow. For all other scenarios, any particle collision on a boundary sticks the particle without the possibility of re-emerging, because the surfaces of the facility were assumed to be easily wetted. For the resuspension scenario, the surface roughness, ε, was 5.0×10^{-5} m, and the lift and adhesion forces were equations 1 and 2 respectively.

3.4 Simulation Scenarios

The parameters and uncertainties described in the above sections were used to create a set of variations from the base simulation. Table 3 lists the simulation number and their variations on individual parameters. The suffix "B" denotes the boiling entrainment mechanism, while the suffix "R" denotes the resuspension entrainment mechanism. Only one resuspension simulation was performed as the parameters and form for the model have yet to be verified to be accurate for this scenario. The injection height is the distance above the pool surface where the parcels are birthed, and the duration is the duration of the boiling regime (i.e. as the time over which particles are injected).

Table 3 Entrainment Scenarios.

Run	Sim. Time (s)	Boiling Duration (s)	Fuel Pool	Injected Mass (kg/s)	Particle Size (um)	Turbulence	Injection Height (mm)	Parcel Temperature (K)
1B	25	17	Gas vel.	8.3×10^{-3}	Dist.	Normal	10	370
2B	35	27	Gas vel.	8.3×10^{-3}	Dist.	Normal	10	370
3B	25	17	Gas vel.	8.3×10^{-3}	Dist.	High	10	370
4B	25	17	Gas vel.	4.15×10^{-3}	Dist.	Normal	10	370
5B	25	17	Gas vel.	1.25×10^{-2}	Dist.	Normal	10	370
6B	25	17	Gas vel.	8.3×10^{-3}	Dist.	Normal	5	370
7B	25	17	Gas vel.	8.3×10^{-3}	Dist.	Normal	10	361
1R	50	17	1D pool, 0.002 m	8.3×10^{-3}	Dist.	Normal	10	370

A text description of each variation is listed in Table 4. The uncertainty of the boiling duration and height are represented in 2B, where boiling is extended from 17 seconds to 27 seconds, while 4B and 5B alter the fuel height from the base 2 mm to 1mm and 3 mm respectively. Scenario 3B increases the turbulence intensity from 20% to 100%. The particle injection height was another unknown, so 6B lowered the injection height to 5 mm. Uncertainty existed as to the exact temperature of the volatile component in each parcel, so the temperature of the particles was lowered to 361K in scenario 7B. Scenario 1R was the resuspension scenario, which experimentally ran for 4.8 hours, but was modeled for 20 additional seconds in the simulation.

Table 4 Entrainment Simulation Variations.

Case	Variation from Baseline
1B	Baseline. 25 second simulation, 10 mm particle injection height, particle size distribution, empty pan (high lip) mesh, 370 K particle injection temperature, and gas velocity representing the fuel pool.
2B	Simulated for 35 seconds with particle injections from 3 to 30 seconds.
3B	Turbulence parameter increased to 100%
4B	Fuel pool height lowered to 1 mm.
5B	Fuel pool height increased to 3 mm.
6B	Particles injected at 5 mm above the bottom of the fuel pan.
7B	Particle injection temperature decreased to 361 K
1R	Resuspension mechanism. 50 second simulation 1D pool model, 2 mm fuel height, 50 μm surface roughness.

4. RESULTS AND DISCUSSION

The filter location in the original experiment and the outflow model boundary are closely situated, meaning the accumulated mass on this surface is representative of the experimentally collected mass.

4.1 Multiple Species Entrainment

The contaminant mass deposition on various surfaces is plotted as a function of time for the baseline scenarios in Fig. 3. Figure 4 displays the number deposition prediction. Deposition values become constant shortly after the particle injections stop at 20 seconds as the suspended mass finishes depositing. The majority of the particles emitted during the boiling phase are predicted to deposit back on the pool or the pool lip. Some deposit on the walls of the facility, but more find their way out of the facility to the model 'outflow' boundary.

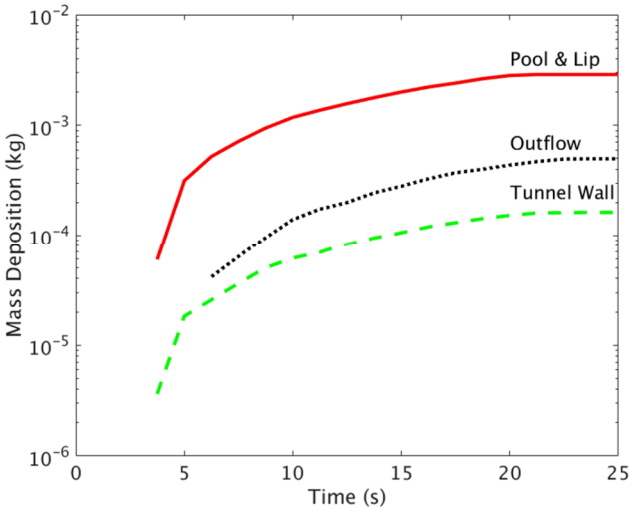

Fig. 3 Boiling: Predicted contaminant mass deposition vs time (1B).

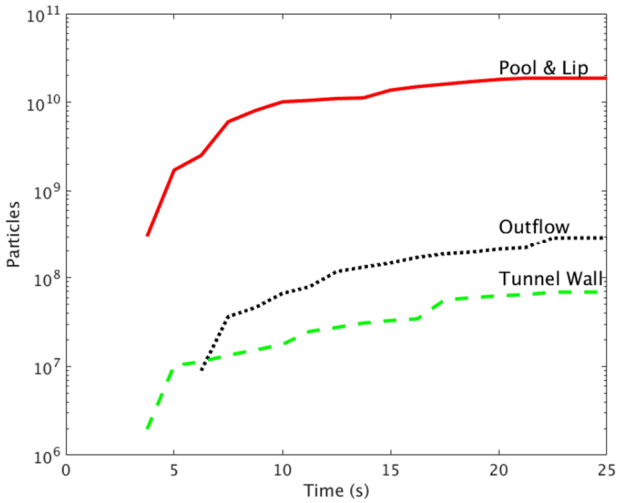

Fig. 4 Boiling: Predicted number deposition vs time (1B).

Figures 5 and 6 display the predicted final mass location for the heptane fuel and the uranium dioxide contaminant respectively. For the heptane fuel, only a portion of the injected fuel is deposited, while the rest evaporates in the flow. Of the deposited mass, the majority settles back onto the pool surface, followed by a significant percentage being deposited onto the pool lip. Less than 0.2% of the deposited fuel is located on the walls or outflow, so representation of this is omitted from the figure. The majority of the contaminant similarly deposits on the fuel pool, followed by the pool lip. However, a significant portion of the contaminant collects on the tunnel walls and outflow. More contaminant deposits on the outflow compared to the previous work that did not model the multi-component evaporation of the particles. In the current work, the fuel component of the particles is seen to evaporate quickly, leaving the smaller solid contaminant particles more susceptible to the flow due to enhanced entrainment of smaller particles in air flows. Previously, only 0.6% of the injected mass deposited on the outflow, compared to 5% here.

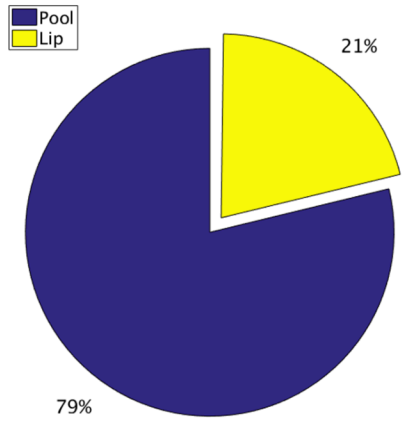

Fig. 5 Predicted mass fate for heptane; boiling case 1 (1B).

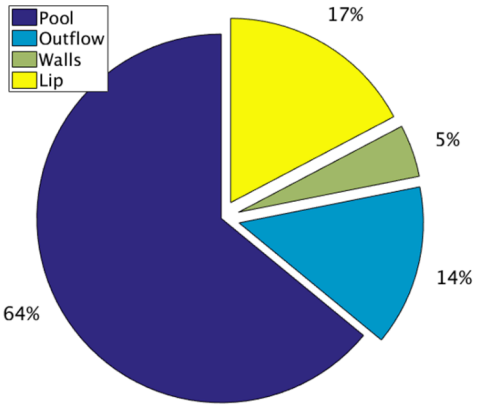

Fig. 6 Predicted mass fate for the contaminant; boiling case 1 (1B).

The final deposition breakdown of the contaminant for all scenarios is shown in Fig. 7. The values were calculated by comparing the deposited contaminant mass on the various surfaces to the total deposited contaminant mass.

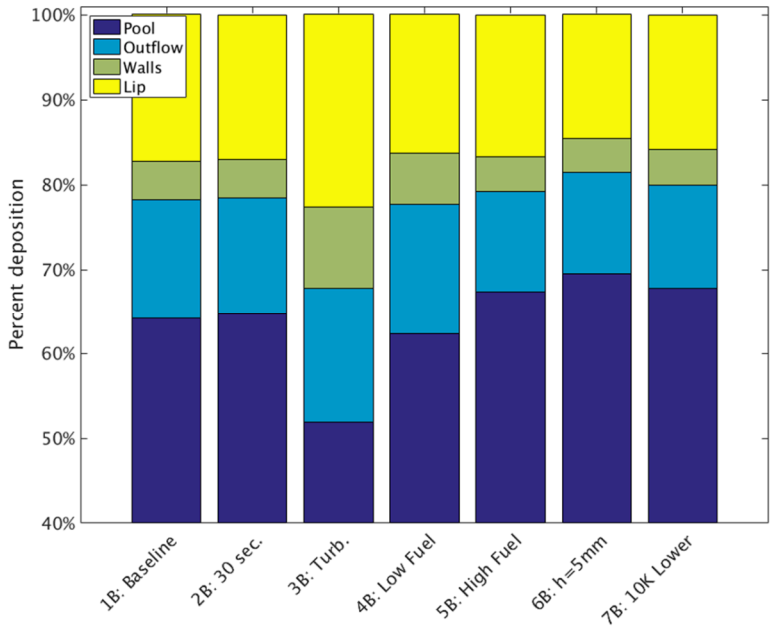

Fig. 7 Predicted contaminant boiling atomization entrainment scenario: UO_2 mass deposition.

Comparing case 2B to 1B shows that the surface deposition percentages do not change appreciably with an increased boiling time. As seen in the previous work, increasing the turbulent intensity increases the percent of contaminant deposited on the lip, walls, and outflow. Particle transport is affected by the turbulence parameters through a continuous random walk model the mimics the effect of sub-grid eddies. Lowering the fuel height (4B) did not significantly alter the deposition percentages, while raising it (5B) slightly increased the deposition on the lip and pool surfaces. Lowering the injection height (6B) increased the pool deposition mass. Lowering the temperature assigned to each particle at the injection time (7B) slightly increased the amount of contaminant deposited on the pool while lowering the outflow deposition percentage. Of the parameters varied, the results were most sensitive to the turbulence parameter variations.

Figure 8 displays the predicted airborne release fractions for the various scenarios alongside the reported experimentally determined release fraction. Lacking certain experimental feature information such as turbulence conditions, boiling duration and inflow velocity contributed to the discrepancy between experimental and predictive values.

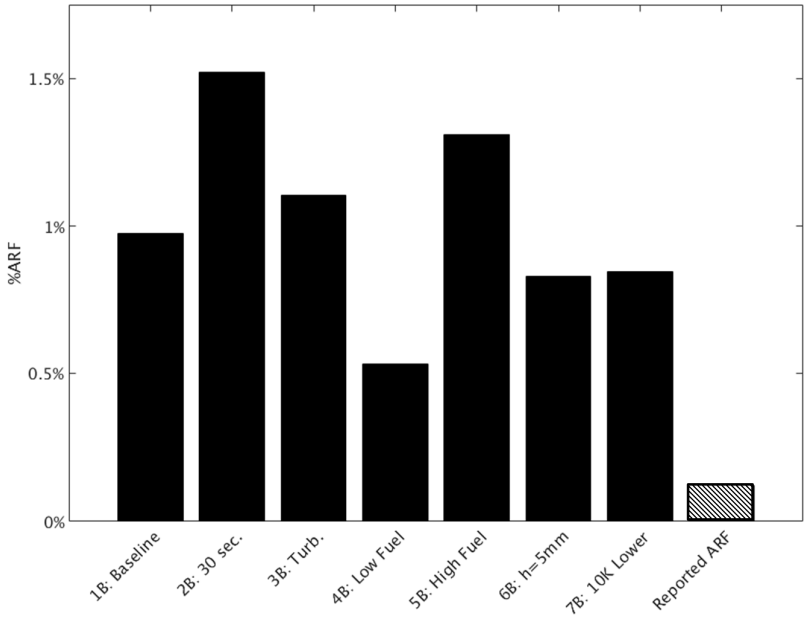

Fig. 8 Predicted and Reported Airborne Release Fraction.

Comparing to the previous work, the majority of the scenarios presented here involving multiple species particle tracking result in higher ARF values than those seen in the single component scenarios. While this deviates more from the reported ARF, the multiple species involve increased physical fidelity. The increase in ARF was expected, since the volatile fuel evaporates off from the particle surface, leaving the significantly smaller solid contaminant. The reduced particle diameter enables a greater percentage of contaminate to entrain into the flow and pass through the outflow boundary, while the previous work saw more particles descend back to the pool surface. In comparison with experimental data, our simulations with multi-component evaporation model predict higher ARF.

4.2 Resuspension Entrainment

The newly implemented resuspension capability results are included in this simulation. While particles resuspend (Fig. 9), outflow contaminant levels did not change in the additional 20 seconds of simulation time. Given a longer simulation time and with tuned resuspension parameters, additional contaminant would be expected at the outflow boundary. Particles were observed to leave the pool, lip, and wall surface; however, they were only observed to redeposit nearby.

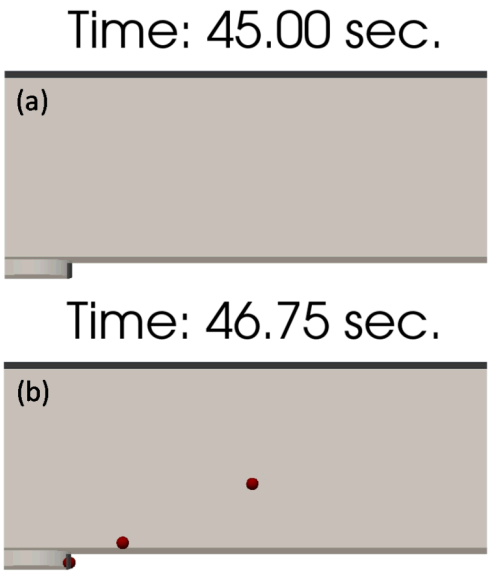

Fig. 9 Resuspension mechanism: (a) all particles have adhered to surfaces or exited the domain, and (b) resuspended particles have re-entered the flow. Particle size is exaggerated for visibility.

The mass departure and addition rates from the various surfaces were not found to be linear in the simulation time, and therefore no attempt was made to predict entrainment. While a simulation prediction of the experimental resuspension entrainment was not successful in this work, the framework exists and was shown to be capable of providing such a prediction.

5. GENERAL DISCUSSION

Including the multi-component particle capability in this study provided significant insight into the entrainment dynamics observed in the boiling scenarios. Observing that the volatile fuel component evaporates rapidly, the solid, non-volatile contaminant is seen to entrain through the outflow in higher volumes, as the smaller particle size is more easily suspended in the flow. If a particle escaped the pool, above the lip, the contaminant would likely entrain and deposit on either the tunnel walls or the outflow.

An effort to determine the resuspension entrainment contribution to the ARF did not provide the anticipated level of insight, but the capability was shown to be functional. One consideration is that the resuspension model presented here is formulated for solid particles. No consideration towards the adhesive force from the surface tension is included.

As in the previous work, the time duration of boiling appears to be the most critical of parameters in determining the entrainment for the boiling mechanism. A boiling time of less than 5 seconds is projected from existing simulation results to match the experimental results. A separate project is currently working on developing a volumetric model for a burning liquid fuel layer using a volume of fluid model. This effort may produce a model that can be used in the future to quantify boiling times.

The distribution of the solid contaminant was ignored in this work, as the precise distribution is unknown. A drop including multiple contaminant particles was predicted to behave as a single particle with an aggregate spherical dimension of contaminant. The contaminants are thought to settle to the bottom of the fuel pool in the physical experiment. In this work, there was no way to assess the distribution of particles in the fuel, so the fuel was assumed to have a uniform contaminant distribution equal to the initial distribution. This subtle feature may be significant to the ARF for these scenarios, and needs to be evaluated in more detail than was found in historical experimental work.

Varying the turbulence parameters was shown to result in significant uncertainty in the deposition locations. Precise modeling of turbulence remains a modeling challenge for CFD scenarios, however the large uncertainty assumed is bracket by the experimental uncertainty due to a lack of reporting of turbulence in the experimental work. This omission could be resolved by additional tests with a closer focus on providing adequate boundary condition descriptions for model predictions.

6. CONCLUSIONS

- Multiple entrainment mechanisms were presented as potential methods for hazardous contaminant release from contaminated fuel fires.
- The predicted ARF calculated by a CFD code was compared to the ARF measured in a relevant historical experiment and previous computational work. The addition of multiple species evaporation and deposition for particles provided new insight to the entrainment dynamics. The volatile fuel was seen to evaporate rapidly in the fire above the pool surface, increasing the likelihood that the remaining non-volatile solid contaminant would transport down the wind tunnel and reach the outflow.
- Practical assumptions for the turbulence boundary conditions result in significant uncertainty in the ARF.
- Boiling mechanism duration was again found to be the most significant factor in predicting the ARF. Improved modeling of particle entrainment from pool boiling will help quantitative accuracy of this type of modeling.
- The particle input temperature did not significantly alter the volatile evaporation, resulting in similar contaminant release.
- Future work would include longer duration simulations of the resuspension of deposits left from a multiple component boiling entrainment scenario in order to detect contaminant release at the collection point, potentially enabling a prediction of the resuspension entrainment ARF.

ACKNOWLEDGMENT

This work is being funded by DOE NSRD Program under WAS Project No. 2015-AU30-SNL-DOE H 3010. Sandia is a multiprogram laboratory operated by Sandia Corporation, a Lockheed Martin Company, for the United States Department of Energy's National Nuclear Security Administration under Contract DE-AC04-94AL85000. Heeseok Koo and Lindsay Gilkey graciously provided technical review of this report.

NOMENCLATURE

ρ_g	gas density	(kg/m^3)	τ_w	wall shear stress	(kg m^{-1} s^{-2})
ρ_f	fluid density	(kg/m^3)	r	particle radius	(m)
j_g	superficial gas velocity	(m/s)	ε	surface roughness	(m)
j_{fe}	superficial liquid drop velocity	(m/s)	K	turbulent kinetic energy	(J)
α	particle lift coefficient	(-)	ε_{turb}	turbulent dissipation	(-)
A_p	particle cross-sectional area	(m^2)			

REFERENCES

[1] Department of Energy, "DOE HANDBOOK: Airborne Release Fractions/Rates and Respirable Fractions for Nonreactor Nuclear Facilities", Volume 1 and 2, U.S. Department of Energy, DOE-HDBK-3010-94, Raffirmed 2013, (2013).

[2] Mishima, J., and Schwendiman, L.C., "The Fractional Airborne Release of Dissolved Radioactive Materials During the Combustion of 30 Percent Normal Tributyl Phosphate in a Kerosine-Type Diluent,"BNWL-B274, June 1973.

[3] Brown, A.L., and Louie, D. L. Y., "Contaminant Entrainment in a Liquid Fuel Fire," Proceedings of the 1st Thermal and Fluid Engineering Summer Conference, TFESC, New York City, USA, August 9-12, 2015. SAND2015-1360C.

[4] Louie, D. L.Y., Brown, A.L. and Restrepo, L., "Computer Capability to Substantiate DOE-HDBK-3010 Data," Proceeding of the 2015 Annual ANS Meeting, San Antonio, TX, June 7-11, 2015.

[5] Mishima, J., Schwendiman, L.C., "Some Experimental Measurements of Airborne Uranium (Representing Plutonium) in Transportation Accidents, BNWL-1732, August, 1973.
[6] Brown, A. L., Zepper, E. T., Louie, D. L. Y., Restrepo, L. "Contaminant Entrainment from a Gasoline Pool Fire," SAND2015-7185C, September 2015, Sandia National Laboratories.
[7] Drysdale, An Introduction to Fire Dynamics, Second Edition, John Wiley & Sons, Inc., 1998.
[8] Sierra Thermal Fluids Development Team, "Sierra Fuego User Manual – Version 4.40," Sandia National Laboratories, SAND 2016-4157, (2016).
[9] Kogan, V., Schumacher, P.M., "Plutonium release fractions from accidental fires," Nuclear Technology, 61, pp. 190-202, (2008).
[10] Bagul, R.K., D. S. Pilkhwal, P.K. Vijayan, and J.B. Joshi, "Entrainment phenomenon in gas-liquid two-phase flow: A review," Sadhana, 38(6), pp. 1173-1217, (2013).
[11] Mishima, J., Schwendiman, L.C., and Radasch, C.A., "Plutonium Release Studies IV. Fractional Release from Heating Plutonium Nitrate Solutions in a Flowing Air Stream," BNWL-931, UC-41 Health & Safety, November 1968.
[12] Derakhti, M., and Kirby, J.T., "Bubble entrainment and liquid-bubble interaction under unsteady breaking waves," J. Fluid Mech. 761, 464-506, 2014.
[13] Borkowski, R., Bunz, H., and Schoeck, W., "Resuspension of Fission Products during Severe Accidents in Light-Water Reactors, KfK3987, EUR 10391, May (1986).
[14] Kataoka, I., and Ishii, M., "Mechanistic Modeling and Correlations for Pool-Entrainment Phenomenon," NUREG/CR-3304, ANL-83-37, April (1983).
[15] Roberts, J.D., Jepsen, R.A., and James, S.C., "Measurements of Sediment Erosion and Transport with the Adjustable Shear Stress Erosion and Transport Flume," Journal of Hydraulic Engineering, Vol. 129, No. 11, 2003.
[16] Lick, W.J., Sediment and contaminant transport in surface waters, Taylor & Francis, 2009.
[17] Sehmel, G.A., "Deposition and Resuspension," Chapter 12 in "Atmospheric Science and Power Production," Randerson, D., editor, DOE/Tic-27601, 1984.
[18] Henry, C., Minier, J.-P., "Progress in particle resuspension from rough surfaces by turbulent flows," Progress in Energy and Combustion Science, 45, pp. 1-53, (2014).
[19] Young, M. F. "Liftoff model for MELCORE," SAND2015-6119, 2015, Sandia National Laboratories.
[20] Pierce, F., Brown, A. L., Louie, D. L. Y., Zepper, E. T., "Multicomponent Evaporation Effects on Particulate Release in a Liquid Fuel Fire," Proceedings of the 2nd Thermal and Fluid Engineering Conference, April 2-5, 2017, Las Vegas, NV, USA, TFEC-IWHT2017-17668.
[21] Magnussen, B.F., "On the Structure of Turbulence and a Generalized Eddy Dissipation Concept for Chemical Reactions in Turbulent Flow," 9th AIAA Sc. Meeting, St. Louis, (1981).
[22] Tieszen, S.R., Domino, S.P., and Black, A.R., "Validation of a simple turbulence model suitable for closure of temporally-filtered Navier-Stokes equations using a helium plume," SAND2005-3210, June 2005, Sandia National Laboratories.
[23] Brown, A.L., Vembe, B.E., "Evaluation of a model for the evaporation of fuel from a liquid pool in a CFD fire code," Proceedings of the ASME International Mechanical Engineering Congress & Exposition, November 5-10, 2006, Chicago, IL, USA, IMECE2006-15147.